Reconstruction of impacts on a composite plate using fiber Bragg gratings (FBG) and inverse methods

Reference:
Rezayat A., De Pauw B., Lamberti A., El-Kafafy M., Nassiri V., Ertveldt J., Arroud G., Vanlanduit Steve, Guillaume P..- Reconstruction of impacts on a composite plate using fiber Bragg gratings (FBG) and inverse methods
Composite structures - ISSN 0263-8223 - 149(2016), p. 1-10
Full text (Publisher's DOI): https://doi.org/10.1016/J.COMPSTRUCT.2016.03.065
To cite this reference: http://hdl.handle.net/10067/1341420151162165141

Accepted Manuscript

Reconstruction of impacts on a composite plate using fiber Bragg gratings (FBG) and inverse methods

A. Rezayat, B. De Pauw, A. Lamberti, M. El-Kafafy, V. Nassiri, J. Ertveldt, G. Arroud, S. Vanlanduit, P. Guillaume

PII: S0263-8223(16)30227-6
DOI: http://dx.doi.org/10.1016/j.compstruct.2016.03.065
Reference: COST 7363

To appear in: *Composite Structures*

Reconstruction of impacts on a composite plate using fiber Bragg gratings (FBG) and inverse methods

A. Rezayat[a,*], B. De Pauw[a,b], A. Lamberti[a], M. El-Kafafy[a,f], V. Nassiri[c], J. Ertveldt[d,a], G. Arroud[a], S. Vanlanduit[a,e], P. Guillaume[a]

[a] *Vrije Universiteit Brussel (VUB), Acoustics and Vibration Research Group (AVRG), Belgium*
[b] *Vrije Universiteit Brussel (VUB), Brussels Photonics Team (B-phot), Belgium*
[c] *University of Leuven (KUL) & Universiteit Hasselt, I-BioStat, Belgium*
[d] *Vrije Universiteit Brussel (VUB), Department ELEC, Belgium*
[e] *University of Antwerp, Op3Mech Research Group, Belgium*
[f] *Helwan university, Cairo, Egypt*

Abstract

Composite materials are nowadays widely used in several applications, especially in the aerospace field. Despite the numerous advantages that composites can offer, the health monitoring of this type of structures is challenging. A major challenge regards the detection and monitoring of delaminations. In the case of aeronautical structures, delaminations are often caused by impacts with external objects. Therefore, the capability of detection, localization and reconstruction of occurring impacts becomes an essential health monitoring tool for the estimation of the remaining structure lifetime. In this paper, we propose a new procedure for the reconstruction of impacts, based on the structural model and on measured vibration data. The procedure is tested over a carbon fiber reinforced composite plate, instrumented with surface mounted fiber Bragg grating sensors. The experimental results show that the proposed algorithm (VS-LS) can localize and reconstruct the impact forces with at least three times better accuracy than the classical pseudo-inverse method.

Keywords: Force identification, impact detection, modal analysis, inverse problem, composite plate, fiber Bragg grating (FBG).

1. Introduction

The use of composite materials has been growing rapidly in the past decade, because of the higher mechanical properties that these materials offer (stiffness/density). Composites are, for instance, light and strong, and therefore they are widely used in aeronautical applications. Despite the numerous existing non-destructive techniques (NDT), damage detection mechanisms over composite materials are much more complex and require more effort and sophisticated hardware. This makes the monitoring and lifetime cycle estimations more difficult for this type of structures. In addition to that, the establishment of maintenance schedules in the framework of structural health monitoring (SHM) becomes often challenging for complex structures.

Composite structures are vulnerable to internal damages, such as delamination and fiber breakage. Most of the internal flaws occur inside the composite material and they might not be visible for inspection from outside [1]. In the particular case of aeronautical structures, impacts of birds or other foreign objects can lead to a degradation of the structural integrity. A typical example of this decrease in structural integrity is the delamination of the composite layers caused by concentrated impact forces.

Damages caused to the composite structures by low velocity impacts are not easy to identify, since no visual deterioration is made to the structure. Therefor, it is useful to try to identify the possible causes of the damage, i.e. the

*Corresponding author
Email address: ali.rezayat@vub.ac.be (A. Rezayat)

forces. The reconstruction of the load signature on structures is a helpful procedure that can considerably help for SHM. When the applied dynamic forces are known, the monitoring will be easier and the maintenance costs will be reduced.

Force identification using structural vibration data has recently attracted a lot of interest. The inverse load identification using system responses is used for monitoring purposes in civil engineering and structural mechanics. In the particular case of aeronautical structures for example, the force identification becomes applicable in impact detection. The impact force reconstruction is a popular application of load identification, in which the location and the amplitude of the impact forces are estimated. Given the structural model, inverse techniques offer the possibility to reconstruct the system's input (forces) from measured vibration data (outputs).

In general, the load identification problem consists of localising the forces, and reconstruction of the force time history. In the literature, the force identification approaches can be divided into two major categories, depending on the applications (see below).

In the first approach, the aim is only to detect the impact. This approach relies mostly on the knowledge of wave propagation in the structure. The time of arrival (TOA) is one of the most popular methods in this category. The use of triangulation techniques and cross correlations can improve the impact localization [2]. Despite the advantages that these techniques offer, most of the time-based methods fail on complex structures. They are highly sensitive to noise, and thus not suitable for identifying colored-band excitation. When the material properties are not known exactly, or when the material in anisotropic, the analytical models usually become non-realistic, so the identification fails [4–12]. In presence of anisotropic materials (such as most of fiber reinforced composites), the wave propagation occurs at different speeds and directions. This makes the force identification process more challenging, since time-based methods require the knowledge of material properties, such as fiber directions, layups, number of layers, etc.

The second approach consists of estimating not only the location but also the applied force history on the structure. The use of a structural model (either in time or frequency domain) is necessary in this approach. The model can be analytical (for simple geometries), experimental or an updated finite element model. Most of these methods are based on optimization techniques. They try to minimize the error between the measured and predicted vibration data, obtained from the calculation of the structural model. The model based methods are not limited to impact detection. They are generally less computationally effective comparing to the TOA techniques. But, with some special considerations, their computation speed can be in the same order of magnitude as TOA methods [15–24].

Model-based techniques have the ability to deal with structures having complex geometry and material composition. In inverse model-based methods, the structure model is perceived as a black box by the algorithm, containing several inputs and outputs. The force identification procedure becomes independent from the geometrical and physical properties of the structure. As composite structures are often composed of complex layer configurations, model-based approach seems to be advantageous than the one based on time. Nevertheless, it is worth mentioning that, if the model is not reliable in the description of the system dynamics, these methods will not be able to produce correct load estimations (ex. changes in the boundary conditions, temperature, damage, etc.)

Both approaches require measuring the vibration of the structure under test. Piezoelectric-based accelerometers are commonly used for vibration measurements. It is possible that in some cases, such as relatively small and light structures, these sensors affect the structure dynamics by their (non-negligible) mass and dimensions. The vibration of the structure can be measured instead by using fiber Bragg gratings (FBG). The use of FBG sensors has increased considerably due to the inherent advantages of optical fibers, such as low weight and the immunity to electromagnetic interference. This type of sensors can measure strain, and they have been used for detecting forces and damages on composite structures [2, 3, 13, 14]. The numerous advantages of FBG sensors make them highly desirable for aerospace applications.

In this paper, we propose a new procedure called variable selective least squares (VS-LS), for localizing and reconstructing single point forces on structures. It consists of a model-based identification approach, that uses the measured strain signals together with the strain frequency response functions (SFRF), in order to estimate the applied forces.

Although the method is limited to single point force identification, it is not restricted to broadband excitations. As the computation time has always been an issue for the inverse load identification techniques, a strong focus is put on the simplicity and robustness of the proposed algorithm. Furthermore, the effect of sensor configurations and model parameters will be investigated in details. The studied structure consists of a fiber re-enforced composite plate (2D structure). The plate is excited using a hammer and the vibration data is measured by FBG sensors. The proposed algorithm has been successfully validated with the experimental data.

The remainder of this paper is structured as follows. In section 2, we will state the inverse problem, described as a set of system of linear equations in frequency domain. This is followed by the theoretical background of the applied methods. Section 3 introduces the experimental setup. The experimental validation of the proposed approach will be illustrated and discussed in section 4. Finally, the section 5 includes the conclusions of the present study. A complete list of the notations used in this paper is presented in the Appendix section.

2. Theory

This section introduces the theoretical background on the fiber Bragg grating (FBG) sensors used for the vibration measurement procedure and on the proposed solution method.

2.1. FBG sensing principle

A fiber Bragg grating (FBG) is a particular type of sensor created in an optical fiber. A grating is inscribed inside the fiber core (Figure 1) by means of UV light. Within the grating region, the index of refraction undergoes a periodic modulation and therefore acts as a wavelength selective filter.

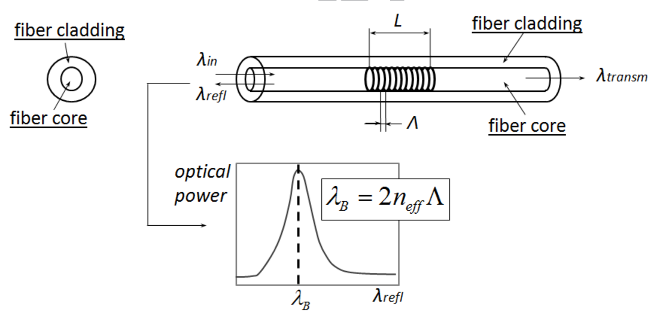

Figure 1: Schematic representation of a FBG. The grating has length L and pitch Λ and is created inside the core region of the optical fiber. The Bragg wavelength λ_B depends on the effective refractive index n_{eff} and on Λ.

When light with a broadband spectrum enters the fiber, the grating reflects one particular wavelength. This wavelength is called the Bragg wavelength λ_B and is given by the following equation:

$$\lambda_B = 2\, n_{\mathrm{eff}}\, \Lambda \tag{1}$$

where, n_{eff} is the effective refractive index averaged over the entire grating length L and Λ indicates the grating pitch (Figure 1). A shift of the Bragg wavelength λ_B occurs when changes in either or both n_{eff} and Λ happen. In isothermal conditions, a strain variation ΔS acting along the fiber axis induces a wavelength shift $\Delta\lambda_B$ which is given by:

$$\Delta\lambda_B = \lambda_B\,(1 - p_{\mathrm{eff}})\,\Delta S \tag{2}$$

where $p_{\mathrm{eff}} = \frac{{n_{\mathrm{eff}}}^2}{2}\,[p_{12} - \upsilon(p_{11} + p_{12})]$, p_{11} and p_{12} are the components of the fiber-optic strain tensor and υ is the Poisson's ratio. For GeO_2 doped (quartz) fiber a typical value of the effective photo-elastic coefficient p_{eff} is 0.204 [25]. It is worth to notice that the assumption of isothermal conditions is realistic when dealing with vibration measurements, since the measurement time is short enough to assume all temperature fluctuations negligible. From Equation 2 it is clear that the internal axial strain acting on the fiber can be retrieved by tracking the Bragg wavelength shifts $\Delta\lambda_B$. For this purpose, different techniques have been proposed in literature.

In this work, we used the so called fast phase correlation (FPC) algorithm recently introduced in [26, 27]. The choice of the FPC algorithm was driven by the need of accurate and precise dynamic strain measurements. It has been proven, in fact, that compared to other techniques the FPC allows to achieve better performance especially when the wavelength resolution is poor and/or the FBG reflected peak is noisy or partially distorted. Moreover, in case of dynamic strain measurements where the strain frequency response function need to be computed, the FPC guarantees higher SNR ratios. A complete discussion on the FPC algorithm can be found in [26–28].

2.2. Preliminary study

As mentioned in the introduction, this study is performed in the frequency domain, and it requires the strain frequency response functions (SFRF) of the structure. The experimental procedure of obtaining the SFRF is presented in Figure 2. For this purpose, the roving hammer test is performed over the DOFs of the structure. Both the force and strains data are converted to the frequency domain (by Fourier transformation), and then used to compute the raw SFRF. Then, a parametric model is created based on the force and strain measurements. This parametric model of the FRFs has been obtained using the poly-reference least-squares complex frequency domain (pLSCF) estimator, industrially known as Polymax method [30, 31]. The Polymax estimator uses the so-called right matrix fraction description (RMFD) model to represent the measured strain frequency response functions (SFRFs). The model is then estimated by fitting the the measured SFRFs, in a linear least-squares sense. The obtained model is denoted by H^s in the next sections. The H^s matrix relates all the DOFs to all of the FBG sensors, installed on the structure.

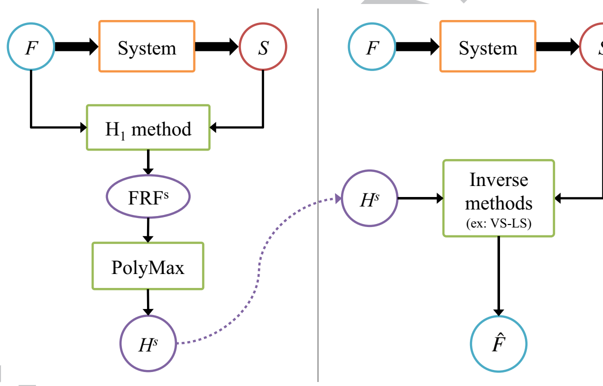

Figure 2: The structural model H^s is obtained in frequency domain. This model will be used together with the strain matrix S in order to estimate the applied force matrix $\hat{F}$.

In another set of measurements, the model H^s will be used together with the vibration measurements S, in order to identify the force vector $\hat{F}$. A 3D representation of the force, strain and the model matrices is illustrated in Figure 3. The third dimension shown in this figure is related to the frequency axis (N_f). The matrices S and F contains all the strain and force data. Each elements of these matrices (S_n^f, F_k^f) corresponds respectively to the strain value of sensor n, and the unknown force at k-th DOF, at frequency f. Each element $H^{s}{}_{n,k}^{f}$ links the DOF k to the sensor n, at frequency f. Note that in this case, the size of S matrix is smaller than the unknown force vector F. This reflects the ill-posed character of the inverse problem. In other words, there are less sensors attached on the structure than the number of unknown variables.

2.3. Problem statement

As described in section 2.2 and Figure 3, the mathematical problem is described as a set of complex linear equations, linking the outputs (strains S^f) to the inputs of the system (force F^f). By means of some inverse procedures, we aim at localizing and reconstructing the applied impact forces. The system dynamics H^s is represented for each frequency line $f \in \{f_1, \ldots, f_{N_f}\}$. The system is described as follows:

$$S^f = H^{sf} F^f \tag{3}$$

where S^f is the $n \times 1$ strain vector with n the number of FBG sensors, F^f is the $k \times 1$ force vector with k the number of unknown force locations, and H^{sf} is the $n \times k$ strain frequency response function (SFRF) model. The H^{sf} matrix, which describes the behavior of the system to external excitations, is obtained experimentally by the roving hammer test (H_1 method: broadband excitation by hammer [29]). In this study, we consider the cases with $n \leq k$, which means that there are less sensors than the unknown force locations (under-determined problem). The solution of the problem ($\hat{F}^f$) is expected to have a sparse pattern, since the impact force is located at one point. In the next section, a new procedure of force identification is introduced in details.

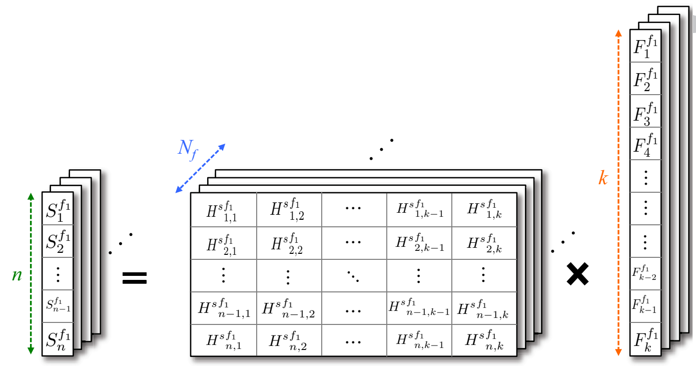

Figure 3: A 3D representation of the matrices S, F, and H^s over frequency. Note that the size of sensors S is smaller than the unknown force locations F.

2.4. Solution method

As mentioned in the previous section, the force identification problem is defined as a 3D system of equations, involving every frequency line N_f inside the band of interest (see Figure 3). The solution of this problem can be estimated for each frequency line, using least squares (LS) as follows:

$$\hat{F}^f_{LS} = \text{argmin}_{F^f} \left\{ \frac{1}{2} \| H^{sf} F^f - S^f \|_2^2 \right\} \tag{4}$$

Since the number of rows in H^{sf} is less than the number of columns ($n < k$), the problem in (4) is ill-posed. Nevertheless, the Pseudo-inverse method still can provide an estimation of the LS solution, since in our case there are more sensors than the number of forces [32].

$$\hat{F} = [H^{sf}]^+ S \tag{5}$$

where the pseudo-inverse operator is represented with $\bullet^+$ operator. Although the solution provided by the pseudo-inverse method is mathematically correct, it usually fails to represent sparse force vectors. Since this technique is estimating a LS solution, the force results are spread over almost all force candidate locations k, and the impact can not be correctly reconstructed. In the literature, there are several methods in which the sparsity of the force vector is guaranteed by imposing more restrictions on the cost functions. The challenge with inverse problems is that they are often mathematically ill-posed, due to the fact that their system model is rank deficient and the condition number is relatively high. There is no unique and general purpose solution method in solving inverse problems.

It is possible to regularize the solution by adding extra constraints or penalty functions, as in [33]. In [34], authors propose a mixed penalty function to promote sparsity in the solutions. Other possible solutions are the Bayesian methods as in [35] or the ℓ_1-norm based cost functions, like in [16]. Although these techniques provide accurate point force identifications, they need a relatively high computation time. In the applications where the calculation speed is a necessary feature, it is better to avoid large scale optimization procedures.

There are several online techniques such as in [4–10] that are fast in the computation. Usually, these methods are designed to detect and localize impacts, and not to reconstruct the force time history, since most of them are not model based. There is a need for a new approach that is model based, and fast enough that allows the system to be used in real-life applications.

We propose a new procedure to localize and reconstruct the impact force. The method is named variable selective least squares (VS-LS). The procedure is defined in the following steps:

- A frequency domain model of the structure is built based on measurement data. $\rightarrow H^{sf}$
- For each frequency line, the k candidate force locations are selected one by one, and each time a force at that location is calculated. $\rightarrow \tilde{F}_k^f$
- The cost function (CF_k) is calculated over all the frequency lines. $\rightarrow CF_k$
- The $\hat{k}$ is obtained by the cost function CF_k.
- When the impact is localized at $\hat{k}$, the model is reduced to the impact DOF ($\rightarrow H^{sf}_k$), and the impact force is estimated.
- The force is reconstructed in time domain by using the inverse Fourrier transform.

VS-LS method

Problem:

$$\text{Find } F \text{ such that:} \quad S = H^s F$$

Solution

$$\text{For } k = 1 : N_d$$
$$\text{For } f = f_1 : f_N$$
$$\tilde{F}_k^f = [H^{sf}_k]^+ S^f$$

$$CF_k = \sum_{f=f_1}^{f_N} \| H^{sf}_k \tilde{F}_k^f - S^f \|_2$$

$$\hat{k} = \text{argmin}_k \{CF_k\}$$
$$\hat{F}^f = [H^{sf}_{\hat{k}}]^+ S^f$$

As the presented procedure examines each DOF separately, the sparsity in the solution vector $\hat{F}$ is guaranteed. The algorithm is not computationally expensive. As the large scale optimization problem is reduced to a simple minimization procedure, a very fast computation is expected. Another advantage of this force identification procedure is that it is not limited to impact forces. As long as a single force is present, the algorithm can identify the location and amplitude of any force spectrum (not limited to broadband forces).

3. Experimental setup and procedure

To illustrate the applicability of the proposed approach, several experiments are conducted. A composite plate (fiber reinforced) with a rectangular shape is clamped from four corners. The plate is composed of 16 plies, with the following layup: [0/90/0/90]2s. This composite plate has a symmetric and balanced layup (same amount of each layer direction). The tensile modulus of the plate is included in the Table 3, together with additional specifications. The structure is a general-purpose composite plate that was selected for the test setup without any particular preferences in material and size selection. It has been fabricated by the R-G company and it is used for the sake of validating the impact identification procedure.

The vibration data (consisting of strain signals) are measured FBG sensors. There are 10 FBG sensors (Ge-doped type I, DTGs from FBGS Int., with wavelength near 1550 nm), equally distributed on a single fiber (blue rectangles in Figure 4). The coordinates of the sensors are presented in Table 2.

The locations and directions of the FBG sensors are chosen arbitrarily. In fact, different sensor configurations have been considered (spiral, rectangular, zigzag, etc.) and they were all studied in order to obtain better signal to noise ratios on the strain signals. Because of the minimum allowed curvature radius of the optical fiber, some technical limitations were encountered. To avoid any damage on the fiber, we decided to select a very straight and simple sensor layout. This allows having some FBGs in 0^o and some other in 90^o. The last FBG is arbitrarily glued at 45^o. The impact identification results show that even with a non-optimized FBG sensor layout, the algorithm is still capable of localizing and reconstructing the impact force. In general, as long as the strain levels are above $1\mu\epsilon$, the strain signals can be correctly measured and the proposed algorithm will work. If the sensors are not located in the nodal points (at resonance frequencies), the chance is high to obtain good signal to noise ratios.

The fiber is attached to the plate surface using a UV curable glue. Only the sensing part of the fiber is glued, allowing to relieve the strain between the individual gratings and avoid cross-talk of the gratings. Figure 5 shows a more detailed view of the setup.

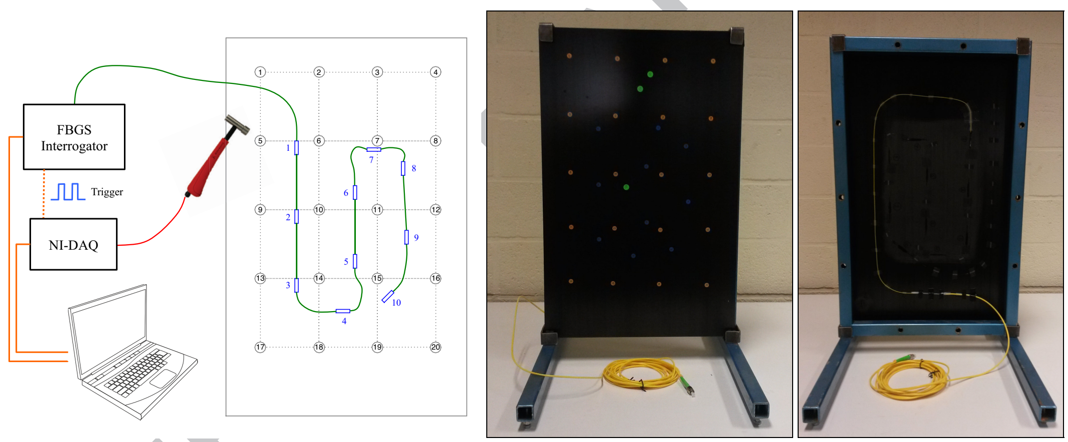

(a) Setup (b) Front view (c) Rear view

Figure 4: The setup consists of a composite plate, instrumented by FBG sensors. The orange dots correspond to the DOFs. The vibration (strain) is measured using FBG sensors, presented by blue dots.

The plate is excited using a PCB® hammer on the DOFs of the plate (orange dots in Figure 4). The applied force is also measured for validation purposes. The hammer force is measured by a National Instruments® data acquisition device (NI-DAQ). As shown in Figure 4, the output strain signal from the fiber sensors is measured with the FBG Scan 700 (from FBGS Int.). The strain measurement is synchronized with the force measurements, by means of a square trigger signal, created with the NI-DAQ. The NI-DAQ acts as the central reference unit for the synchronization of all the 11 measurements (1 force and 10 strains). The strain measurements are triggered using the intercepted output trigger signal of NI-DAQ. All the input (force) and output (strains) signals are triggered with the NI-DAQ reference. The strain signals are derived from the Bragg wavelengths shifts that are determined using the FPC algorithm. An example of raw input and output measurement data is illustrated in Figure 6.

Using the set-up explained in the previous paragraph, the system model is first constructed experimentally following, following the system identification techniques presented in [30, 31, 36]. In this way, an input-output model is

ACCEPTED MANUSCRIPT

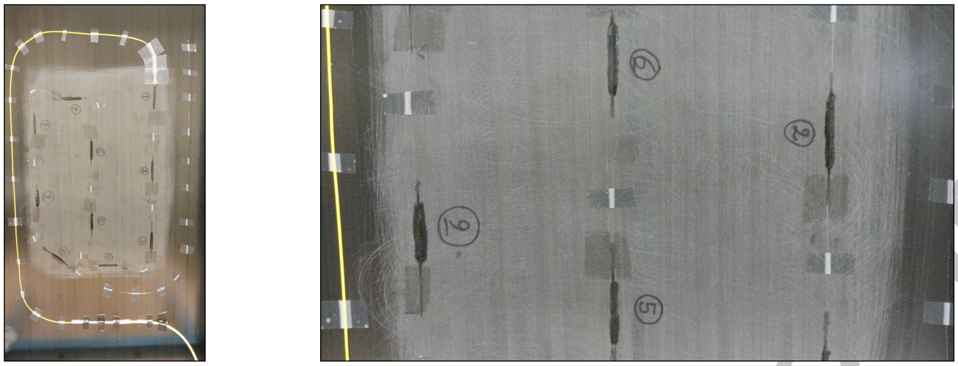

(a) Sensor configuration (b) Zoom view

Figure 5: The 10 FBG sensors are attached to the plate as shown in (a). A zoom view in (b) shows an example of the sensor configuration.

calculated based on the measured strain signals. Then, system identification techniques are applied to the measured SFRF in order to find the modal parameters of the system. This SFRF relates the output strains to the input point forces. The working frequency range is limited up to 250 Hz. Each measurement was performed for a total duration of 4.5 s, with a sampling frequency of 1 kHz. Figure 7 shows some of the SFRF over the selected frequency range.

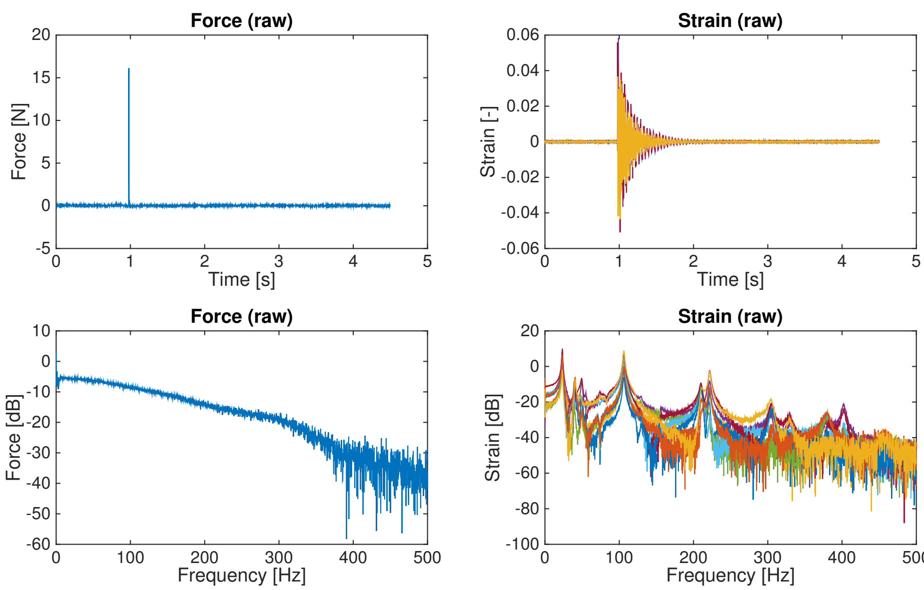

Figure 6: An example of the raw data, measured during the experiments (impact at location 11). The hammer force and all of the FBG strain signals are stored and transformed to frequency domain.

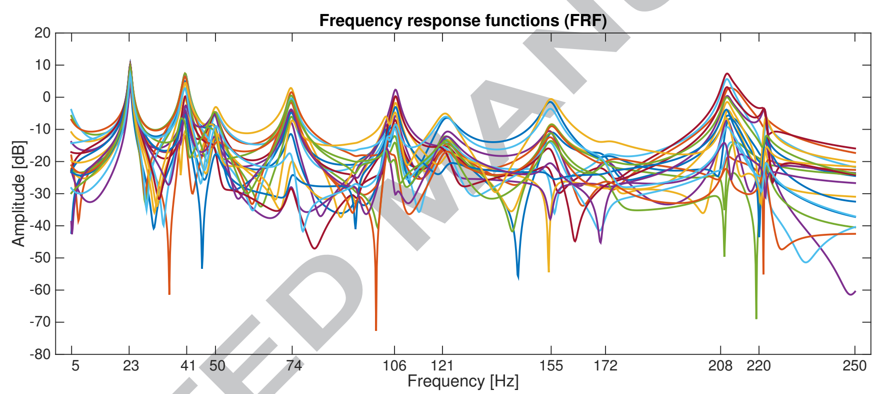

Figure 7: This figure shows some of the SFRF curves, related to the first sensor. The (approximate) resonance frequencies are emphasized in the *x*-axis.

4. Results and discussion

4.1. Forward verification

The verification of the quality of the system model (H^s) is a necessary condition for obtaining reliable results in the inverse procedure. This verification consists of comparing the measured strains with the estimated strains that are computed using the structural model H^s. The results of the forward check show that in general, a very good overall agreement between the measured and simulated response signals is obtained. As this condition is satisfying, the model H^s can be used in the inverse calculation for force reconstruction.

$$S_e = H^s F \tag{6}$$

where F and S represents the measured force and strain. The estimated strains S_e will be compared to the actual strains on the structure S. Some results of the forward check are presented in figures 9. As the comparison study shows a good overall agreement is observed between the measured and estimated strain signals. The quality of this fit indicates the relevance of the structural model.

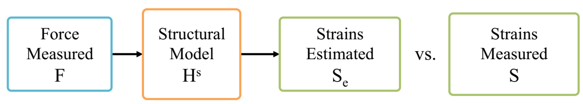

Figure 8: The estimated strains are calculated based on the structural model and a measured force.

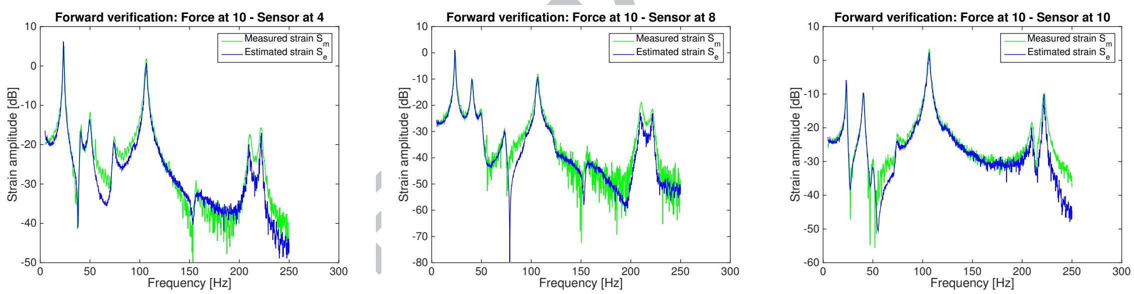

(a) Sensor 4 (b) Sensor 8 (c) Sensor 10

Figure 9: The measured and estimated strains show a good overall agreement. In this case, the force is applied at location 10.

4.2. Force identification

The force identification on the composite plate is performed using both the classical pseudo-inverse and the new procedure, as described in section 4.2. The inputs of the algorithm consist of the structural model H^s obtained in the previous sections, together with the strain measurement matrix S, measured during an experiment. To illustrate the efficiency of the suggested algorithm, three different load cases are considered. The results of the force identification procedure are shown in Figure 10.

The first study case corresponds to the case where the point 2 is impacted. All the FBG sensors contribute to the measured strain vector. The purpose of analyzing this case is to validate the proposed procedure. In the second study case, the force is applied at point 11, and only six FBG sensors (1 3 5 7 9 10) are active. In this way, the effect of sensor number on the result quality is examined. The last study case pushes the sensor constraints to their limits, where only three FBG sensors are taken into account in the inverse process (1 4 9). For the last case study, the plate is impacted at point 17.

It is more convenient for illustration purposes to make use of a non-dimensional parameter called β, that can provide a better geometrical understanding of the force localization. This parameter is defined as suggested in [37], and consists of a normalization over frequency and DOFs.

$$\beta_i = \frac{\sum_{f=f_1}^{N_f} \|F_i^f\|_2^2}{\sum_{j=1}^{k} \sum_{f=f_1}^{N_f} \|F_j^f\|_2^2} \qquad i, j \in \{1 \cdots k\} \tag{7}$$

Among the results presented in Figure 10, the amplitude of β for each DOF is represented by a color (see the colorbar). In the last column, the values of the cost function CF are plotted per force point, calculated following the formulae in section 4.2. The location $\hat{k}$ that minimizes CF will be identified as the impact location.

Once the force location is identified, the system model is reduced to the localized point ($H^{sf}_{\hat{k}}$), and the force amplitude is calculated. The last step of the force identification process consists of reconstructing the time history of the localized force using inverse Fourier transform. The time domain results are presented in Figure 11. The relative error is also calculated for each case, in order to provide a basis for the comparison of different methods.

$$RE = \frac{\|F - \hat{F}\|_2}{\|F\|_2} \tag{8}$$

Table 1: The computation time and the relative error (RE), corresponding to each case study. This table shows the quality of the estimations made by VS-LS method.

	Computation time [s]			Relative error (RE) [-]		
	Case 1	Case 2	Case 3	Case 1	Case 2	Case 3
Pseudo-inverse	0.49	0.36	0.33	1.35	7.52	1.57
VS-LS	0.73	0.74	0.71	0.64	0.71	0.32

For each study case, the plot of $\beta_{imposed}$ shows the exact loading conditions of the composite plate. As illustrated in this figure, a general trend can be observed in the results provided by pseudo-inverse technique: this method fails to identify the correct force location. These results are in agreement with the theoretical expectations. Since the pseudo-inverse provides a LS solution of the problem, it lacks the sparsity feature that is necessary in this particular case (point forces). On the other hand, the VS-LS method localizes the impact force correctly. The plot of the cost function CF confirms the localization capabilities of this technique. As explained in the previous sections, the VS-LS estimates a sparse solution of the force vector F. The reconstructed force in time domain (in all study cases) is in agreement with the measured applied force (see Figure 11).

Although the poor localization capability of the pseudo-inverse method, it still remains the faster than VS-LS in the computation time. As shown in Table 1, the pseudo-inverse is at least 2 times faster than VS-LS, but they are both less than a second. The reconstructed forces by VS-LS in time domain have a better agreement with the measured forces. In all the studied cases, the force time history matches the exact one. VS-LS not only localizes the force locations, but provides also very good estimations of the applied force.

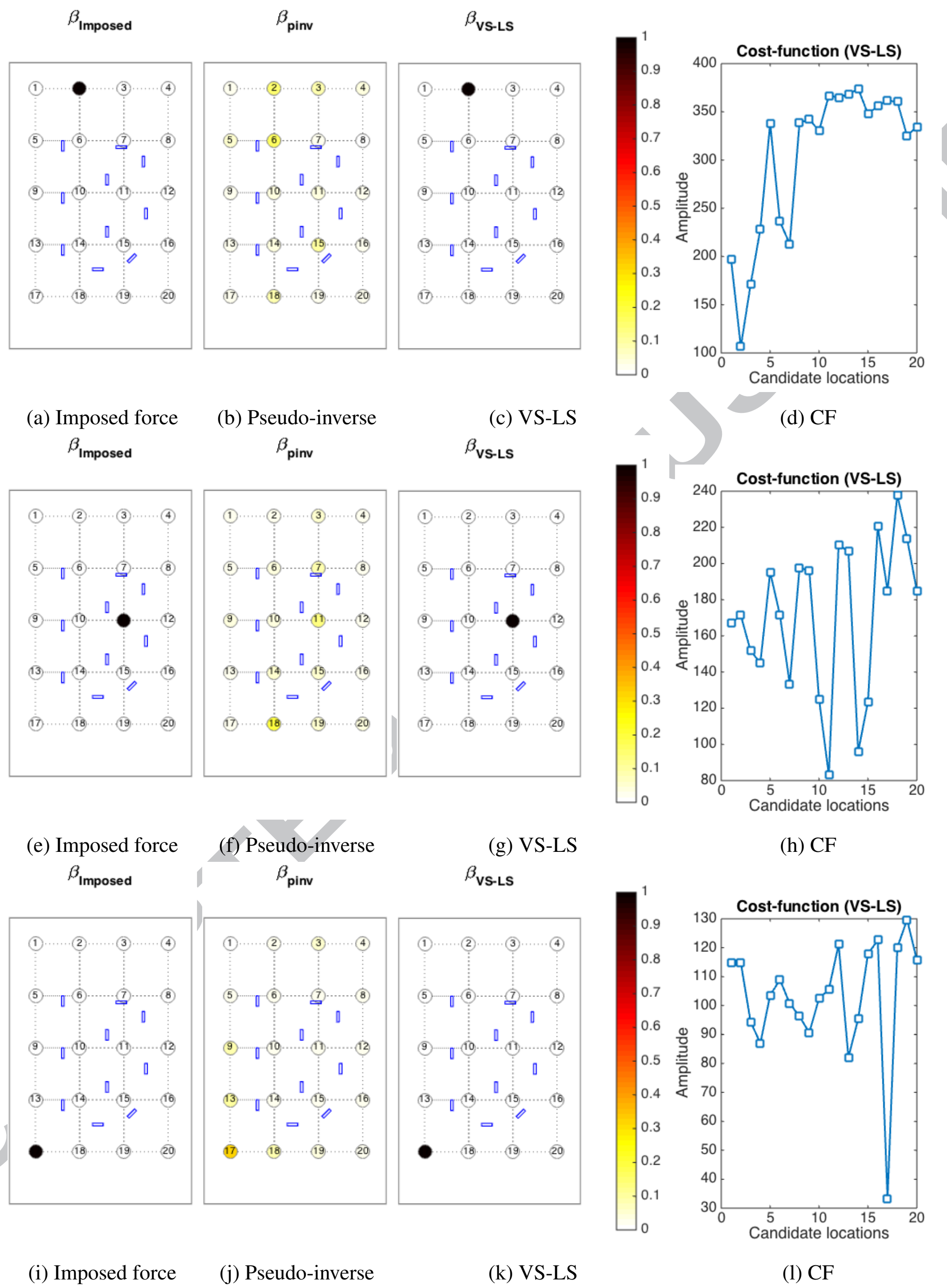

Figure 10: Some results of the force identification procedure are presented at this figure. Figures (a), (b), (c) and (d) correspond to a force at location 2 and consider all the 10 FBG sensors. Figures (e), (f), (g) and (h) correspond to a force at location 11 and consider FBG sensors at [1 3 5 7 9 10]. Figures (i), (j), (k) and (l) correspond to a force at location 17 and consider FBG sensors at [1 4 9].

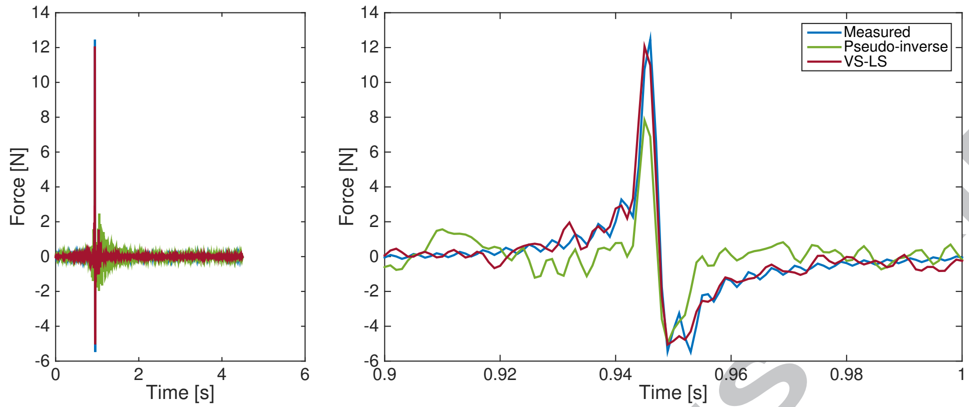

(a) Case 1: Force at point 2

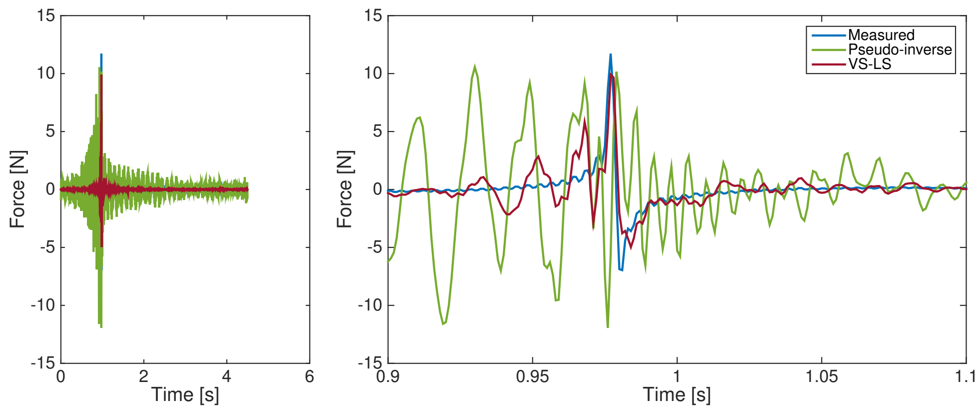

(b) Case 2: Force at point 11

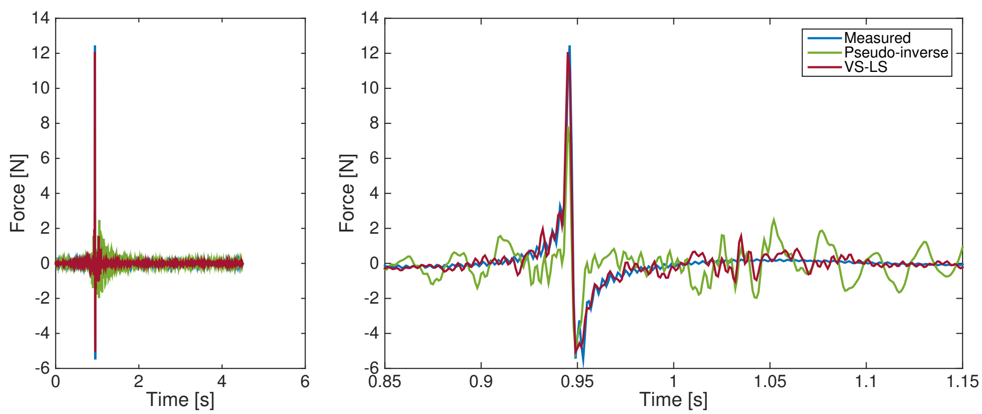

(c) Case 3: Force at point 17

Figure 11: The applied forces are reconstructed in time domain for each test case. The zoom views in the figures show a better estimation quality for VS-LS method. Note that only the force vector at the excited point is plotted. The force signals are band-filtered between 5-250 Hz.

5. Conclusion

In this study, the point force reconstruction has been addressed, and a new procedure is introduced for solving the ill-conditioned load identification problem. Impacts have been applied to an instrumented composite plate, in several test cases. The strain data is measured using optical fibers (FBG), attached on the surface of the plate. The location of the applied forces are determined by minimizing a cost function. The forces are then reconstructed in time domain. The comparison of the results from the pseudo-inverse and the newly proposed method shows that the classical methods fail to produce good force estimations. The experimental results indicate that the proposed technique (VS-LS) is able to correctly identify the applied impacts on the plate.

Acknowledgments

The research presented in this paper has been performed within the framework of the project G.0738.11 "Inverse identification of wind loads on structures", funded by the Research Foundation Flanders (FWO), Belgium. Their financial support is gratefully acknowledged. The authors appreciate the support received the Flamish Agency fo Innovation by Science and Technology (IWT) for the SBO project grant 120024 (SSC). The authors also acknowledge the contributed help of R. Daitov on the implementation and application of algorithms, as part of the master thesis project.

Appendices

$\hat{\bullet}$	Estimated matrix
$\bullet^T$	Conjugate transpose operator
$\|\| \bullet \|\|_p$	ℓ_p-norm defined as $\sqrt[1/p]{\sum_i \bullet_i^p}$
$\bullet^+$	Pseudo-inverse of a matrix
f	Frequency
N_f	Number of frequency lines in the studied range
n	Number of sensors (equations in the problem)
k	Number of candidate force locations (unknowns in the problem)
L	Length of the grating
Λ	Grating pitch
f_{eff}	Effective refractive index
Λ_{in}	Incident wavelength
Λ_{refl}	Reflected wavelength
Λ_{transm}	Transmitted wavelength
Λ_B	Bragg wavelength
p_{eff}	Effective photo-elastic coefficient
p_{ij}	Components of the fiber-optic strain tensor
υ	Poisson ratio
β	Normalized force index (indicating the force location)
S	Strain matrix $n \times 1 \times N_f$
F	Force matrix $k \times 1 \times N_f$
$\hat{F}$	Estimated force matrix $(k * N_f) \times 1$
H^s	Frequency response function matrix in 3D $n \times k \times N_f$
H_k^{sf}	The k-th column of the frequency response function at a given frequency f
DOF	Degree of freedom
SFRF	Frequency Response Function
LS	Least Squares estimation
UV	Ultra violet
CF	Cost function
RE	Relative error
FBG	FIber Bragg grating

Table 2: The composite plate is instrumented with 10 FBG sensors attached at following coordinates. The reference point is placed at lower left corner of the plate.

Sensor	x-coordinate [cm]	y-coordinate [cm]	Angle [deg]
1	10.0	38.2	90
2	10.0	28.5	90
3	10.0	18.5	90
4	16.2	15.5	0
5	18.5	21.5	90
6	18.5	31.7	90
7	20.5	38.5	0
8	25.5	35.4	90
9	26.0	25.4	90
10	23.2	16.5	45

Table 3: The specifications of the composite plate.

Layers	[0/90/0/90]2s
Height	550 mm
Length	350 mm
Thickness	2.4 mm
Fiber volume	60%
Density	1.6 g/cm^3
Tensile strength	1.300 MPa
Tensile modulus	130.00 MPa
Shear modulus	5300 MPa

References

[1] Mangalgiri PD, Composite materials for aerospace applications. Bulletin of Materials Science. (1999) May 1;22(3):657-64, doi:10.1007/BF02749982.
[2] Shrestha P, Kim J-H, Park Y, Kim C-G. Impact localization on composite wing using 1D array FBG sensor and RMS/correlation based reference database algorithm. Composite Structures 2015;125:15969. doi:10.1016/j.compstruct.2015.01.029.
[3] Kahandawa GC, Epaarachchi J, Wang H, Lau KT. Use of FBG sensors for SHM in aerospace structures. (2012) Photonic Sensors, 2(3), 203-214.
[4] Gaul L, Hurlebaus S. Identification of the impact location on a plate using wavelets. Mechanical systems and signal Processing, (1998) ;12:78395. doi:10.1006/mssp.1998.0163.
[5] Morales R, Group A. A new self-calibrated procedure for impact detection and location on flat surfaces, (2013):710420. doi:10.3390/s130607104.
[6] Si L, Baier H. Real-time impact visualization inspection of aerospace composite structures with distributed sensors. Sensors 2015;15:1653656. doi:10.3390/s150716536.
[7] Wu E, Yeh J, Yen C, Method A. Identification of impact forces at multiple locations on laminated plates. Applied Mechanics (1994);32.
[8] Doyle J. Determining the contact force during the transverse impact of plates. Experimental mechanics (1987):6872.
[9] Yang H, Shin TJ, Lee S. Source location in plates based on the multiple sensors array method and wavelet analysis. Mechanical Science and Technology (2014);28:18. doi:10.1007/s12206-013-0938-5.
[10] Yang M. An integrated real-time health monitoring and impact/collision detection system for bridges in cold remote regions, (No. MPC 15-282).
[11] Meo M, Zumpano G, Piggott M, Marengo G. Impact identification on a sandwich plate from wave propagation responses. Composite structures. (2005) Dec 31;71(3):302-6.
[12] Kirkby E, de Oliveira R, Michaud V, Månson JA. Impact localisation with FBG for a self-healing carbon fibre composite structure. Composite Structures (2011) Dec 31;94(1):8-14.
[13] Coelho CK, Hiche C, Chattopadhyay A. Impact localization and force estimation on a composite wing using fiber Bragg gratings, Sensors (2010):85287.
[14] Gomez J, Jorge I, Durana G, Arrue J, Zubia J, Aranguren G, et al. Proof of concept of impact detection in composites using fiber Bragg grating arrays. Sensors (2013);13:119982011. doi:10.3390/s130911998.
[15] Li WM, Wang HD. On the identification technology for the random load spectrums, (2015) International Conference on Electrical, Automation and Mechanical Engineering. Atlantis Press.
[16] Ginsberg D, Fritzen C. New approach for impact detection by finding sparse solution. ISMA, (2014) p. 205164.
[17] Jia Y, Yang Z, Song Q. Experimental study of random dynamic loads identification based on weighted regularization method. Sound and vibration (2015):111. doi:10.1016/j.jsv.2014.12.010.
[18] Qiao B, Chen X, Luo X, Xue X. A novel method for force identification based on the discrete cosine transform. Vibrations and acoustics (2015);137:051012. doi:10.1115/1.4030616.
[19] Las V, Zemcik R, Kroupa T, Bartosek J. Reconstruction of impact force on curved panel using piezoelectric sensors. Procedia Engineering 48 (2012): 367-374. doi:10.1016/j.proeng.2012.09.527.
[20] Gunawan FE. Levenberg-Marquardt iterative regularization for the pulse-type impact-force reconstruction. Sound and vibration (2012);331:542434. doi:10.1016/j.jsv.2012.07.025.
[21] Wang BT, Chiu C-H. Determination of unknown impact force acting on a simply supported beam. Mechanical systems and signal processing (2003);17:683704. doi:10.1006/mssp.2001.1463.
[22] Thiene M, Ghajari M, Galvanetto U, Aliabadi MH. Effects of the transfer function evaluation on the impact force reconstruction with application to composite panels, Composite Structures, Volume 114, August (2014), Pages 1-9, ISSN 0263-8223, http://dx.doi.org/10.1016/j.compstruct.2014.03.055.
[23] Frieden J, Cugnoni J, Botsis J, Gmr T. Low energy impact damage monitoring of composites using dynamic strain signals from FBG sensorsPart I: Impact detection and localization. Composite structures (2012) Jan 31;94(2):438-45.
[24] Sierra-Perez J, Torres-Arredondo MA, Gemes A. Damage and nonlinearities detection in wind turbine blades based on strain field pattern recognition. FBGs, OBR and strain gauges comparison. Composite Structures. (2016) Jan 31;135:156-66.
[25] Barlow D, Payne A. The stress-optic effect in optical fibers. Quantum Electron., 19(1):834839, (1983). ISSN 0018-9197. doi: 10.1109/JQE.1983.1071934.
[26] Lamberti A, Vanlanduit S, De Pauw B, Berghmans F. A novel fast phase correlation algorithm for peak wavelength detection of fiber Bragg grating sensors. (2014) Optics Express, 22(6):70997112, 2014. ISSN 1094-4087. doi: 10.1364/OE.22.007099.
[27] Lamberti A, Vanlanduit S, De Pauw B, Berghmans F. Peak detection in fiber Bragg grating using a fast phase correlation algorithm. (2014), In SPIE Photonics Europe (pp. 91410Y-91410Y). International Society for Optics and Photonics.
[28] Lamberti A, Vanlanduit S, De Pauw B, Berghmans F. Influence of Fiber Bragg Grating Spectrum Degradation on the Performance of Sensor Interrogation Algorithms. (2014), Sensors, 14(12), 24258-24277.
[29] Allemang R J, Brown DL. Experimental modal analysis. VCH Publishers, Inc., Handbook on Experimental Mechanics. Second Revised Edition (USA), (1993), 635-750.
[30] Guillaume P, Verboven P, Vanlanduit S, Van Der Auweraer H, Peeters B. A poly-reference implementation of the least-squares complex frequency-domain estimator. In Proceedings of IMAC, volume 21, pages 183192, (2003).
[31] Peeters B, Van der Auweraer H, Guillaume P, Leuridan J. The polymax frequency-domain method: a new standard for modal parameter estimation. Shock and Vibration, 11(3-4):395409, (2004).
[32] Penrose R. A generalized inverse for matrices. In Mathematical proceedings of the Cambridge philosophical society, volume 51, pages 406413. Cambridge Univ Press, (1955).
[33] Tikhonov AN, Arsenin VY. Solution of ill-posed problems. (1977).

[34] Rezayat A, Nassiri V, De Pauw B, Ertveldt J, Vanlanduit S, Guillaume P. Identification of dynamic forces using group-sparsity in frequency domain. Mech Syst Signal Process 2015. doi:10.1016/j.ymssp.2015.09.015.
[35] Aucejo M. Structural source identification using a generalized Tikhonov regularization. Sound and vibration (2014);333:5693707. doi:10.1016/j.jsv.2014.06.027.
[36] El-Kafafy M, Guillaume P, Peeters B. Modal parameter estimation by combining stochastic and deterministic frequency-domain approaches. Mechanical Systems and Signal Processing, 35(1):5268, (2013).
[37] Parloo E, Verboven P, Guillaume P, Van Overmeire M. Force identification by means of in-operation modal models. Journal of Sound and Vibration, 262(1):161173, (2003).